Designing Air-Core Photonic-Bandgap Fibers Free of Surface Modes

Hyang Kyun Kim, *Associate Member, IEEE*, Jonghwa Shin, *Student Member, IEEE*, Shanhui Fan, Michel J. F. Digonnet, *Associate Member, IEEE*, and Gordon S. Kino, *Life Fellow, IEEE*

***Abstract*—It is known that the coupling of core modes to surface modes in air-core photonic-bandgap fiber (PBF) can give rise to large propagation losses. Using computer simulations, we analyze the relationship between the air-core geometry and the presence or absence of the surface modes in air-core PBFs with a triangular hole pattern. We identify ranges of core radii for which the fiber supports no surface modes over the entire wavelength range of the bandgap, i.e., only core modes are present. In particular, for a hole radius $\rho = 0.47\Lambda$, where Λ is the hole spacing, the core supports a single mode and no surface modes for core radii between 0.8Λ and 1.1Λ. The absence of surface modes suggests that fibers within this range of configurations should exhibit a very low propagation loss. We also show that the existence of surface modes can be predicted quite simply from a study of the bulk modes alone, which is much simpler and faster than carrying out a full analysis of the defect modes.**

***Index Terms*—Bulk modes, core modes, optical fiber, photonic-bandgap fibers, photonic crystal, surface modes.**

I. Introduction

AIR-CORE photonic-bandgap fibers (PBFs) have attracted great interest in recent years due to their unique advantages over conventional fibers: propagation loss is not limited by the core material and holds the promise of being exceedingly low, nonlinear effects are very small, and the air core can be filled with liquids or gases to generate the desired light–matter interaction. Numerous new applications enabled by these advantages have been demonstrated recently [1]–[5]. Calculations of selected properties of the fundamental mode of the PBFs have also been reported [6]–[8].

It has been recently demonstrated that surface modes play a particularly important role in air-core PBFs. A surface mode is a defect mode localized at the terminating edge of the photonic crystal [9]–[14]. In contrast, a core mode is one in which most of the energy is contained within the air core. There is strong experimental and analytical evidence that the fundamental core mode couples to one or more of these surface modes. Since the latter is lossy, this is a source of propagation loss. Furthermore, since surface modes occur across the entire bandgap, no portion of the available spectrum is immune to this loss mechanism. This effect is believed to be the source of the remaining loss ($\sim$13 dB/km) in state-of-the-art air-core PBFs [9]. Understanding the physical origin of surface modes and identifying fiber configurations that are free of such modes across the entire bandgap is therefore of importance in the ongoing search for low-loss PBFs.

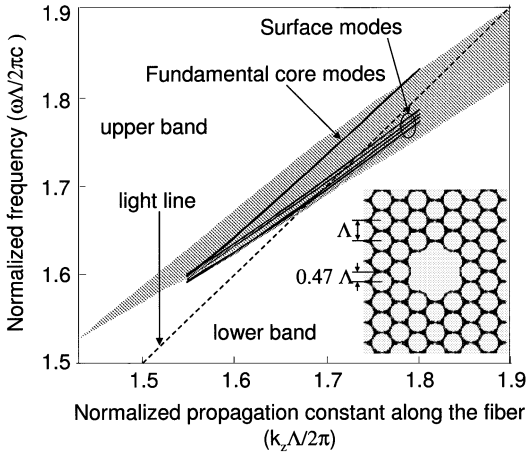

Fig. 1. Dispersion curves of defect modes for a triangular-pattern PBF with an air-core radius $R = 1.132\Lambda$. The shaded area represents the photonic bandgap of the crystal (hole-to-hole spacing $\rho = 0.47\Lambda$).

In this paper, we report the results of a parametric study that investigates in greater detail the properties of both the core modes and the surface modes of PBFs. We have focused our investigation on the most common PBF geometry, namely fibers with a triangular air-hole pattern in the cladding and a core obtained by introducing an air defect [6]–[8]. We propose new geometries with ranges of core diameters for which the fiber supports no surface modes over the entire wavelength range of the bandgap, and only core modes are present. In particular, for fiber radii between 0.8Λ and 1.1Λ, where Λ is the hole-to-hole spacing of the triangular pattern, the core supports a single mode and no surface modes at all. The absence of surface modes suggests that fibers within this range of configuration should exhibit substantially lower losses than current fibers. We also show that the existence of surface modes in the defect structure can be predicted quite simply from a study of the bulk modes alone, which, because the structure is truly periodic, is a much simpler and faster task than carrying out a full analysis of the defect modes.

II. Simulations

We study a PBF with a cladding photonic crystal region consisting of a triangular lattice composed of circular air holes in silica [6]–[8]. The core region is created by introducing a larger air hole of radius R at the center of the fiber. By varying the

Manuscript received September 25, 2003; revised February 3, 2004. This work was supported by Litton Systems, Inc., a wholly owned subsidiary of Northrop Grumman and by an NSF-NRAC grant.

The authors are with the Edward L. Ginzton Laboratory, Stanford University, Stanford, CA 94305-4088 USA (e-mail: kino@stanford.edu).

Digital Object Identifier 10.1109/JQE.2004.826429

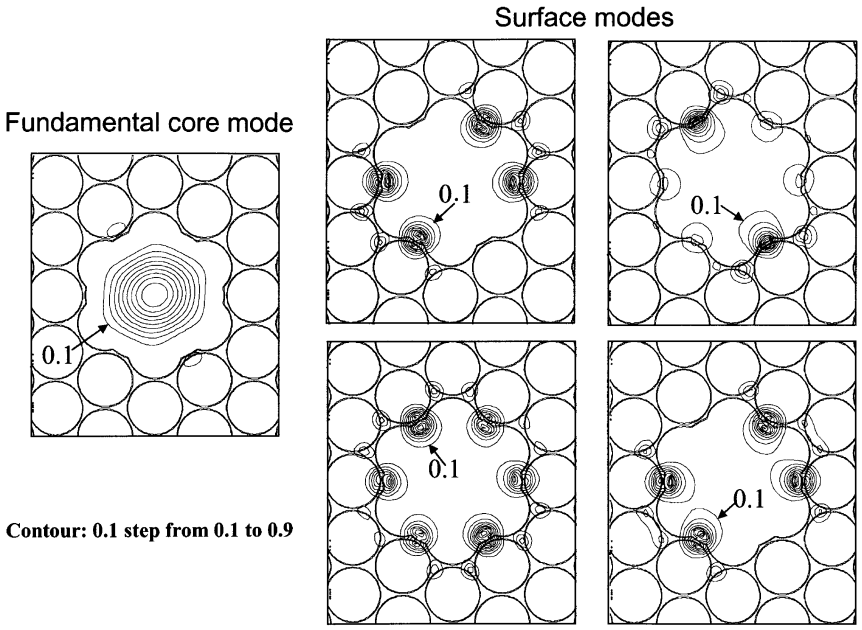

Fig. 2. Intensity contour maps of the fundamental mode and exemplary surface modes of the air-core PBF of Fig. 1.

core radius, we can systematically study the effect of the core radius on the core modes and the effect of surface truncation on the surface mode behavior. Simulations were performed on the University of Michigan AMD Linux cluster of parallel Athlon 2000MP processors using a full-vectorial plane-wave expansion method [15]. We used a grid resolution of $\Lambda/16$ and a supercell size of 8×8. When running the simulations with 16 processors, complete modeling of the electric-field distribution and dispersion curves of all the core modes and surface modes of a given fiber typically took between 7 and 10 h.

For a triangular pattern, we find that a photonic bandgap exists only for air-hole radii ρ larger than about 0.43Λ. The largest circular air-hole radius that can be fabricated in practice is slightly higher than 0.49Λ. We therefore chose to simulate a structure with an air-hole radius between these two extreme values, namely $\rho = 0.47\Lambda$. Although all simulations reported in this paper were carried out for $\rho = 0.47\Lambda$, similar results were obtained for $\rho = 0.49\Lambda$, and the qualitative conclusions of this paper are valid for any air-hole size.

III. Properties of Core Modes

Fig. 1 shows the theoretical ω-k_z diagram of the fiber geometry under study generated for a core radius $R = 1.132\Lambda$. This particular radius was selected because it corresponds closely to a core formed by removing seven cylinders from the center of the PBF, a configuration commonly used in practice (see the inset of Fig. 1) [16]. The vertical axis is optical angular frequency $\omega = 2\pi c/\lambda$ normalized to $2\pi c/\Lambda$, i.e., Λ/λ, where λ is the free-space wavelength, c is the velocity of light in vacuum, and Λ is the photonic-crystal structure period. The horizontal axis is the propagation constant along the axis of the fiber (z direction) k_z, normalized to $2\pi/\Lambda$, i.e., $k_z\Lambda/2\pi$. The first photonic bandgap supported by this infinite structure is represented by the shaded region in Fig. 1. This bandgap depends on the value of ρ (equal to 0.47Λ here), but it is independent of the core dimension. It shows that, in this fiber, the normalized frequencies for which light can be guided in air range from $\sim$1.53 to $\sim$1.9. The dashed line represents the light line, below which no core modes can exist, irrespective of the core size and shape.

The solid curves in Fig. 1 represent the dispersion relations of the core and surface modes. The related intensity profiles of selected modes at $k_z\Lambda/2\pi = 1.7$ are plotted in Fig. 2. These profiles indicate that the highest frequency mode inside the bandgap is the fundamental core mode (topmost curve in Fig. 1). All other modes in the bandgap are surface modes, which have intensity localized at the core-cladding boundary, as shown in Fig. 2. The strength of the spatial overlap with the silica portions of the fiber is different for core and surface modes, which results in the core mode having a group velocity close to c and the surface modes having a lower group velocity (see Fig. 1). Another important distinguishing feature is that the surface modes that fall within the bandgap always cross the light line within the bandgap, whereas core modes never cross the light line, as is well illustrated in Fig. 1.

The behavior of core and surface modes has been investigated as a function of defect size by changing the core radius R from 0.6Λ to 2.2Λ in 0.1Λ steps. Fig. 3 is the ω-k_z diagram of the same fiber geometry as Fig. 1 but plotted for a larger core radius ($R = 1.8\Lambda$). This core shape is illustrated in the inset of Fig. 3. The number of core modes has increased, as expected, but also all the modes are now core modes. As the frequency is increased from the low-frequency cutoff of the bandgap, the highest order core modes appear first, in a group of four or more modes (here four), depending on the core size and mode degeneracy [7]. As the frequency is further increased, the number of modes reaches some maximum number (14 in the case of Fig. 3), and then it gradually decreases to two (the two fundamental modes) at the high-frequency cutoff of the bandgap. The maximum number of

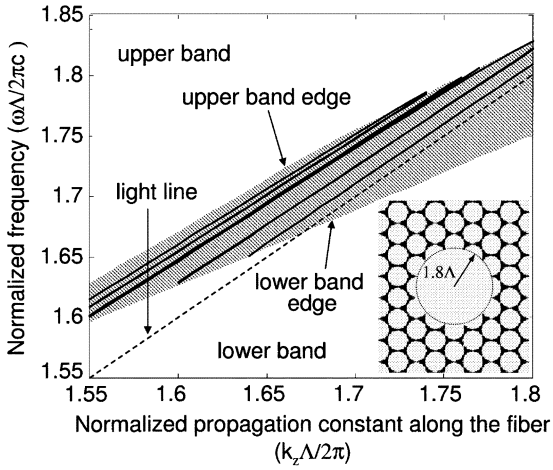

Fig. 3. Dispersion curves of the defect modes for a core radius $R = 1.8\Lambda$.

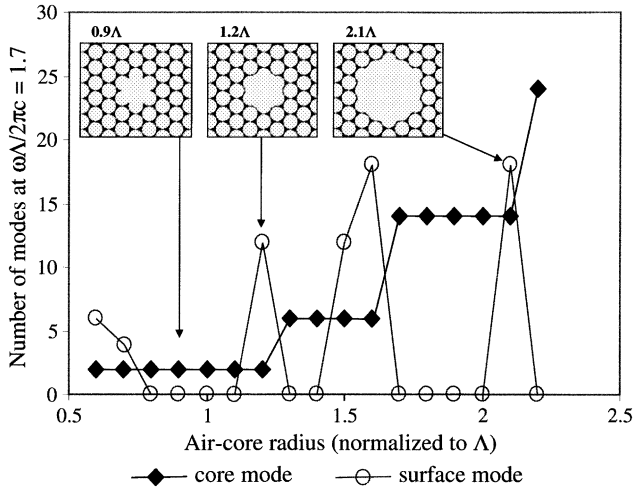

Fig. 4. Number of core modes (diamonds) and surface modes (circles) versus the air-core radius at the normalized frequency $\omega\Lambda/2\pi c = 1.7$. The core shapes for core radii of 0.9Λ, 1.2Λ, and 2.1Λ are shown in the inset.

core modes occurs at or in the vicinity of the frequency where the light line intersects the lower band edge.

Fig. 4 shows the dependence on R of this maximum number of core modes (i.e., the number of modes is plotted at $\omega\Lambda/2\pi c = 1.7$). The number of surface modes is also shown, as well the core shape for representative radii ($R = 0.9\Lambda, 1.2\Lambda$, and 2.1Λ). We find striking similarities between the behavior of the core modes in PBFs and in conventional fibers based on total internal reflection. The fundamental mode, like an LP_{01} mode, is doubly degenerate (see Figs. 1 and 3), very nearly linearly polarized, and it exhibits a Gaussian-like intensity profile [7]. The next four modes are also degenerate, and their electric field distributions are very similar to those of the HE_{21}^{odd}, HE_{21}^{even}, TE_{01}, and TM_{01} of conventional fibers. Many of the core modes, especially the low-order modes, exhibit a twofold degeneracy in polarization over much of the bandgap. As the core radius is increased, the number of core modes increases in discrete steps (see Fig. 4), from two (the two fundamental modes) to six (these two modes plus the four degenerate modes mentioned above), then 14 (because the next eight modes happen to reach cutoff at almost the same radius), and so on.

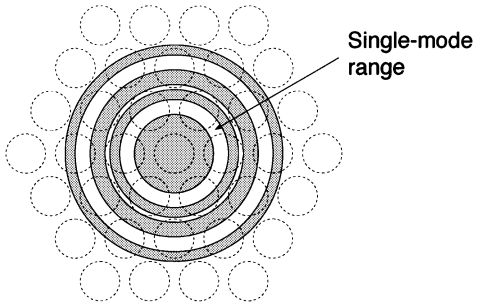

Fig. 5. Graphical representation of the air-core radius ranges that support core modes only (unshaded rings) and both core and surface modes (shaded rings).

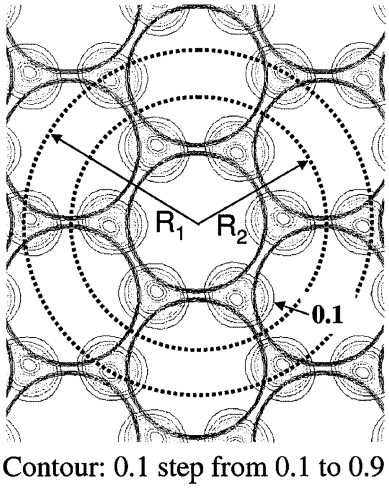

Fig. 6. Intensity contour map of the highest frequency bulk mode below the bandgap at the Γ point. R_1 is an example of a core radius that supports both core modes and surface modes, and R_2 an example of a core radius that supports only core modes.

An important aspect of Fig. 4 is that, when R falls in certain bounded ranges, all modes are found to be core modes. The first three of these ranges are $(\sim 0.8\Lambda$–$\sim 1.1\Lambda)$, $(\sim 1.3\Lambda$–$\sim 1.4\Lambda)$, and $(\sim 1.7\Lambda$–$\sim 2.0\Lambda)$. The case $R = 1.8\Lambda$ illustrated in Fig. 3 is a particular example of a surface-mode-free PBF. These regions are illustrated schematically in Fig. 5, where the background pattern of dotted circles represents the infinite photonic crystal structure, the shaded annular areas represent the ranges of core radii that support surface modes, and the unshaded areas represent the ranges of radii that are free of surface modes (only the first three surface-mode-free rings are shown). In the first of the unshaded ranges ($\sim 0.8\Lambda$ to $\sim 1.1\Lambda$), the core supports a single core mode and no surface modes at all across the entire wavelength range of the bandgap, i.e., the PBF is truly single mode. To our knowledge, this is the first report of a single-mode all-silica PBF design. Examples of terminating surface shapes that fall in this single-mode range are shown in the inset of Fig. 4 ($R = 0.9\Lambda$). It might be possible to manufacture these particular configurations involving small tips of glass protruding into the core using an extrusion method. Most stack-and-draw fabrication techniques, on the other hand, result in a smooth dielectric boundary between the photonic crystal cladding and the air cores.

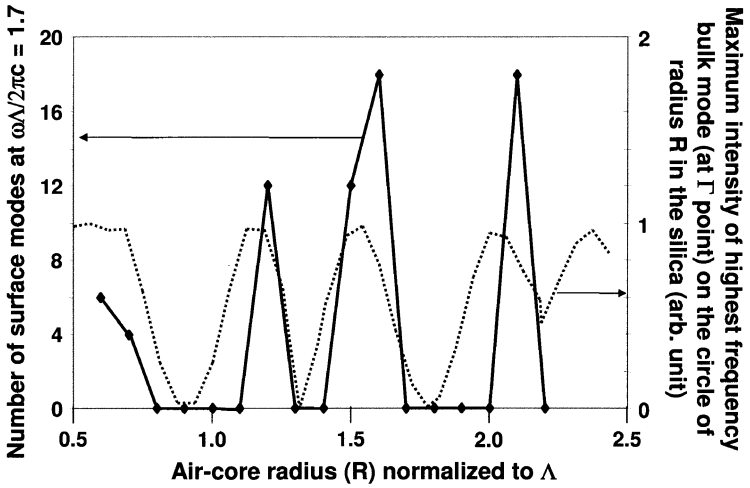

Fig. 7. Dotted curve represents the maximum intensity of the highest frequency bulk mode in the dielectric on a circle of radius R as a function of R (see text). The solid curve is the maximum number of surface modes versus R, reproduced from Fig. 4.

IV. Properties of Surface Modes

The number of surface modes is also strongly dependent on the core radius, albeit in a highly nonmonotonic fashion. For core radii in the vicinity of $\sim 0.6\Lambda$, $\sim 1.2\Lambda$, $\sim 1.6\Lambda$, and $\sim 2.2\Lambda$, many surface modes are introduced, resulting in the peaks in the number of surface modes apparent in Fig. 4. Moreover, in these vicinities, the number of surface modes varies rapidly with R. We note that typical experimental PBFs are fabricated by removing the central 7 cylinders $(R \approx 1.15\Lambda)$ or 19 cylinders $(R \approx 2.1\Lambda)$ to form the core. It is unfortunate that these particular values of R, which happen to be more straightforward to manufacture, also happen to lead to geometries that support surface modes (see Fig. 4). When surface modes are present, it has been shown by Allan *et al.* that the loss is lowest in the frequency ranges where the dispersion curve of the fundamental core mode does not intersect the dispersion curve of any surface mode, and therefore coupling from the core mode to the surface modes is weak [9]. Nevertheless, there is also evidence that residual coupling to surface modes, presumably induced by index profile perturbations, still dominates the loss in state-of-the-art 13-dB/km-loss PBFs [9]. Thus, a first important conclusion of this analysis is that in fibers with cores obtained by removing 7 or 19 central cylinders, the propagation loss is expected to be sizable, as observed in practice. Another key conclusion is that PBFs with core radii in the truly single-mode range identified earlier (R from $\sim 0.8\Lambda$ to $\sim 1.1\Lambda$ for $\rho = 0.47\Lambda$) are expected to exhibit lower losses, and probably substantially lower, than PBFs reported to date, and eventually even lower losses than conventional silica fibers.

Based on the foregoing, it is of fundamental importance to investigate the basic conditions at which surface modes occur and to design new structures for which no surface modes are present. Careful inspection of the unshaded regions in Fig. 5 show that surface modes occur only when the radius R intersects corners of the dielectric, i.e., the portions of the dielectric that are surrounded by three air holes. The existence of surface modes and their behavior in a photonic-crystal structure are known to depend strongly on the termination location of a photonic crystal [11], [13]. Ramos-Mendieta *et al.* [12] reported that terminating an infinite photonic crystal results in the creation of a surface mode satisfying the new boundary condition, which is detached from the bulk mode and moves into the bandgap. We have found that, for the PBFs modeled here, the existence of surface modes is strongly correlated with the amount of perturbation introduced by the air core on the highest frequency bulk mode of the lower band at the Γ point (i.e., $k_x = k_y = 0$). The magnitude of this perturbation scales like the intensity of this bulk mode in the portion of the dielectric intersected by air core. If the core radius is such that the core surface intersects dielectric material where this mode has a high intensity, then the core will support surface modes. To illustrate this point, we show in Fig. 6 an intensity contour map of the highest frequency bulk mode at the Γ point, plotted for $k_z\Lambda/2\pi = 1.7$. Intensity maxima occur at the corners of the silica structure. If we choose the core radius to be R_1 (see Fig. 6), then the core surface cuts through several (six) of these intensity maxima and surface modes are expected to be present. On the other hand, if the core radius is chosen to be R_2, then the core surface does not intersect any intensity maxima and the core should support no surface modes. To validate this argument, we plot in Fig. 7 the maximum intensity of the highest frequency bulk mode in the dielectric on a circle of radius R as a function of R. Also shown is the number of surface modes, reproduced from Fig. 4. These two curves are clearly strongly correlated, which confirms that surface modes occur for radii R such that the edge of the core cuts through the portion of the high-intensity lobes of the highest frequency bulk mode located in the dielectric. This analysis suggests a simple intuitive criterion to quickly predict whether a given fiber geometry supports surface modes, which is to compute the modes of the infinite photonic crystal and to evaluate the spatial overlap between the highest frequency bulk mode's intensity profile and the core surface in the dielectric. This intensity profile takes comparatively little time to be computed, and since it is independent of the core radius it only needs to be calculated once,

so this method is considerably faster than simulating the actual surface modes for a range of core sizes. This design tool can be used conveniently to optimize a photonic-crystal structure and/or the air-core shape in order to avoid surface modes. For the PBF pattern investigated in this study, for example, it predicts that structures with core radii between $\sim 0.8\Lambda$ and $\sim 1.1\Lambda$ support only the fundamental core mode, as demonstrated by exact simulations.

V. Conclusion

We have investigated the surface mode behavior of PBFs, using a triangular lattice cladding structure as a representative example. Surface modes are found to occur in structures where the air core terminates the photonic-crystal cladding at locations in the dielectric near the maximum intensity point of the highest frequency bulk mode of the PBF's lower band. This general criterion, which we believe is applicable to an arbitrary hole pattern, provides a simple method to quickly evaluate whether a PBF with a given geometry supports surface modes and to design PBFs free of surface modes. For the triangular lattice symmetry studied here, and for an air-hole radius $\rho = 0.47\Lambda$, we find that a single fundamental core mode exists for air-core radii in the range of $\sim 0.8\Lambda$ to $\sim 1.1\Lambda$.

Acknowledgment

The authors would like to thank Prof. J. Vuckovic of Stanford University for helpful discussions.

References

[1] B. Temelkuran, S. Hart, G. Benoit, J. D. Joannopoulos, and Y. Fink, "Wavelength-scalable hollow optical fibers with large photonic bandgaps for CO_2 laser transmission," *Nature*, vol. 420, pp. 650–653, 2002.

[2] D. Ouzounov, F. Ahmad, A. Gaeta, D. Muller, N. Venkataraman, M. Gallagher, and K. Koch, "Dispersion and nonlinear propagation in air-core photonic band-gap fibers," in *Proc. Conf. Laser and Electro-Optics (CLEO) 2003*, Baltimore, MD, June 1–6, 2003. paper CThV5.

[3] M. J. Renn, D. Montgomery, O. Vdovin, D. Z. Anderson, C. E. Wieman, and E. A. Cornell, "Laser-guided atoms in hollow-core optical fibers," *Phy. Rev. Lett.*, vol. 75, pp. 3253–3256, 1995.

[4] F. Benabid, J. C. Knight, and P. St. J. Russell, "Particle levitation and guidance in hollow-core photonic crystal fiber," *Opt. Express*, vol. 10, pp. 1195–1203, 2002.

[5] K. Suzuki and M. Nakazawa, "Ultrabroad band white light generation from a multimode photonic bandgap fiber with an air core," in *Proc. Conf. Laser and Electro-Optics (CLEO)*, Pacific Rim, Chiba, Japan, July 2001, paper WIPD1-11M, pp. 15–19.

[6] R. F. Cregan, B. J. Mangan, J. C. Knight, T. A. Birks, P. St. J. Russell, P. J. Roberts, and D. A. Allan, "Single-mode photonic band gap guidance of light in air," *Science*, vol. 285, pp. 1537–1539, 1999.

[7] J. Broeng, S. Barkou, T. Sondergaard, and A. Bjarklev, "Analysis of air guiding photonic bandgap fibers," *Opt. Lett.*, vol. 25, pp. 96–98, 2000.

[8] J. Broeng, D. Mogilevstev, A. E. Barkou, and A. Bjarklev, "Photonic crystal fibers: A new class of optical waveguides," *Opt. Fiber Technol.*, vol. 5, pp. 305–330, 1999.

[9] D. C. Allan, N. F. Borrelli, M. T. Gallagher, D. Müller, C. M. Smith, N. Venkataraman, J. A. West, P. Zhang, and K. W. Koch, "Surface modes and loss in air-core photonic band-gap fibers," *Proc. SPIE*, vol. 5000, pp. 161–174, 2003.

[10] J. D. Joannopoulos, R. D. Meade, and J. N. Winn, *Photonic Crystals: Molding the Flow of Light*. Princeton, NJ: Princeton Univ. Press, 1995, pp. 73–76.

[11] A. Yariv and P. Yeh, *Optical Waves in Crystals: Propagation and Control of Laser Radiation*. New York: Wiley, 1984, pp. 210–215.

[12] F. Ramos-Mendieta and P. Halevi, "Surface electromagnetic waves in two-dimensional photonic crystals: Effect of the position of the surface plane," *Phys. Rev. B*, vol. 59, no. 23, pp. 15 112–15120, 1999.

[13] W. T. Lau and S. Fan, "Creating large bandwidth line defects by embedding dielectric waveguides into photonic crystal slabs," *Appl. Phys. Lett.*, vol. 81, pp. 3915–3917, 2002.

[14] D. Müller, D. Allan, N. Borrelli, K. Gahagan, M. Gallagher, C. Smith, N. Venkataraman, and K. Koch, "Measurement of photonic band-gap fiber transmission from 1.0 to 3.0 μm and impact of surface mode coupling," in *Proc. Conf. Laser and Electro-Optics (CLEO) 2003*, Baltimore, MD, June 1–6, 2003. paper QtuL2.

[15] S. G. Johnson and J. D. Joannopoulos, "Block-iterative frequency-domain methods for Maxwell's equations in planewave basis," *Opt. Express*, vol. 8, no. 3, pp. 173–190, 2001.

[16] J. A. West, N. Venkataraman, C. Smith, and M. T. Gallagher, "Photonic crystal fibers," in *Proc. 27th Eur. Conf. Optical Communications*, Amsterdam, Netherlands, Sept. 30–Oct. 4 2001. paper ThA2.2.

Hyang Kyun Kim (A'01) received the B.S. degree in physics from Yonsei University, Seoul, Korea, in 1987, and the M.S. and Ph.D. degrees in physics from Korea Advanced Institute of Science and Technology (KAIST), Taejon, in 1990 and 1994, respectively.

She has been a Research Associate with Edward L. Ginzton Laboratory, Stanford University, Stanford, CA, since 2002. Her previous affiliations include Senior Research Engineer with the Electronics and Telecommunication Research Institute, Taejon, Korea (1994–1999), Member of Technical Staff, Bell Laboratories, Lucent Technologies (1999–2000), and Principal Staff Engineer, Novera Optics, CA (2001–2002). Her research interest includes various optical parameters affecting the perfomance of optical communication systems, such as polarization effect, nonlinear effect, noise accumulation from the cascaded optical amplifiers, dynamic gain flattening, and the effect of concatenated components. Currently she is working on the investigation of various phenomena of photonic-bandgap fibers such as defect modal analysis, characterization of modal behavior for sensors, and communication applications.

Jonghwa Shin (S'01) was born in Seoul, Korea, in 1980. He received the M.S. degree in electrical engineering from Stanford University, Stanford, CA, in 2003, where he is currently working toward the Ph.D. degree.

In 2001, he worked on the invention of novel all-optical multi-input logic gates in the Optical Communication Systems Laboratory, Seoul National University. He joined the current research group in 2002, and his recent research interests are in the theoretical and computational design and analysis of three-dimensional nanophotonic structures.

Mr. Shin is a student member of the Optical Society of America. He is the receipint of a scholarship from the Korea Foundation for Advanced Studies and is one of the first recipients of the Samsung Lee Kun Hee Scholarship.

Shanhui Fan received the Ph.D. degree in theoretical condensed matter physics from the Massachusetts Institute of Technology (MIT), Cambridge, in 1997.

He has been an Assistant Professor of electrical engineering at Stanford University, Stanford, CA, since 2001. He was a Research Scientist with the Research Laboratory of Electronics at MIT prior to his appointment at Stanford. His research interests are in computational and theoretical studies of solid-state and photonic structures and devices, especially photonic crystals, microcavities, and nanophotonic circuits and elements. He has published 60 journal articles in this field, has given more than 30 invited talks at major international conferences, and currently holds 14 U.S. patents.

Prof. Fan is a recipient of the National Science Foundation Career Award in 2002 and a David and Lucile Packard Fellowship in Science and Engineering in 2003.

Michel J. F. Digonnet (A'01) received the degree of engineering in physics from Ecole Superieure de Physique et de Chimie de la Ville de Paris, the Diplome d'Etudes Approfondies in coherent optics from the University of Paris, Orsay, in 1978, and the M.S. and Ph.D. degrees in applied physics from Stanford University, Stanford, CA, in 1980 and 1983, respectively. His thesis research concerned single-mode fiber couplers and wavelength-division multiplexers, and rare-earth-doped single-crystal fiber lasers and amplifiers.

Until 1986, he was employed by Litton Guidance and Control, Chatsworth, CA, to carry out research as a Visiting Scholar at Stanford University, in the area of miniature solid-state lasers. From 1986 to 1990, he developed fiber delivery systems, high-energy 2-μm flashlamp-pumped solid-state lasers, and human tissue optical sensors for laser angioplasty with MCM Laboratories, Mountain View, CA. Since 1991, he has been a Senior Research Scientist with Stanford University. His current research interests include rare-earth-doped fiber amplifiers, lasers, and superfluorescent sources, third-order nonlinearities in fibers, fiber switches, glass poling for nonlinear switching and modulation, and novel architectures for acoustic fiber sensor arrays. He has chaired many conferences on these subjects, authored 140 articles, and edited a book on rare-earth-doped fiber devices. He has been the principal inventor or co-inventor of 40 issued U.S. patents.

Gordon S. Kino (S'52–A'54–SM'63–F'66–LF'94) received the B.Sc. and M.Sc. degrees in mathematics from London University, London, U.K., and the Ph.D. degree in electrical engineering from Stanford University, Stanford, CA.

He is the W. M. Keck Foundation Professor of Electrical Engineering, Emeritus, and Professor, by Courtesy, of Applied Physics, Emeritus. He was the Director of the Ginzton Laboratory at Stanford University. He has worked on microwave tubes, electron guns, plasmas, the Gunn effect, acoustic devices, acoustic imaging, nondestructive testing, fiber-optics and microscopy; his current interests are in various forms of microscopy, acoustic devices, fiber optics and optical storage. He has written over 430 papers and 47 patents. He and his students have developed new types of scanning optical microscopes and interferometric microscopes, and invented the Real-Time Scanning Confocal Optical Microscope, the Mirau Correlation Microscope, the Solid Immersion Lens for optical microscopy and storage and a Micromachined Confocal Scanning Optical Microscope. At the present time he is developing a new type of dual-axes MEM's microscope for optical endoscopy *in vivo*, and carrying out research on near-field microscopy as well as supervising several students on projects involving acoustooptic fiber sensors and fiber optic devices for communications. He and Timothy Corle are the authors of *Confocal Optical Microscopy and Related Techniques* (New York: Academic, 1996), and he is the author of *Acoustic Waves: Devices, Imaging, and Analog Signal Processing* (Englewood Cliffs, NJ: Prentice-Hall, 1987).

Dr. Kino was a Guggenheim Fellow in 1967 and is currently a Fellow of the American Physical Society and the AAAS and a member of the National Academy of Engineering. In 1984, he was the recipient of the IEEE Sonics and Ultrasonics Group Achievement Award and in 1986 the ASNT Achievement Award in Applied Research.